MNRAS **000**, 1–?? (2019) Preprint 19 July 2019 Compiled using MNRAS LATEX style file v3.0

Dark matter halo shape at $z = 0$ in the Auriga simulations: radial evolution and alignment with the stellar disk

Jesus Prada,[1⋆] Jaime E. Forero-Romero,[1] Volker Springel[2]
[1] *Departamento de Fśica, Universidad de los Andes, Cra. 1 No. 18A-10, Edificio Ip, Bogotá, Colombia*
[2] *Max-Planck-Institut für Astrophysik, Karl-Schwarzschild-Str. 1, D-85741 Garching, Germany*

Accepted XXX. Received YYY; in original form ZZZ

ABSTRACT

We present shape measurements of dark matter halos at redshift $z = 0$ in a suite of 30 zoom-in simulations from the Auriga project. We compare the results in full magneto-hydrodynamics against dark matter only physics. We find a strong influence of baryons in making dark matter halos rounder at all radii compared to its dark matter only counterparts. At distances $\lesssim 30$ kpc, rounder and coherent dark matter distributions correlate with extended massive stellar disks and low gas densities. We measure the alignment between the halo and the stellar disk and find almost perfect alignment at $0.25R_{200} \sim 56$ kpc. In some cases the alignment between the two components significantly changes as a function of radius implying that the halo shape twists; this effect correlates with extended stellar disks and low gas densities and is almost absent in the dark matter only simulations. In a comparison against observational constraints we find that 20% of halos are consistent with observational results derived from the Pal 5 stream that favor $b/a \approx 1$ and $c/a > 0.77$. Including baryons is a required element to achieve this level of agreement. In contrast, none of the simulations (dark matter only and with baryons) can reproduce the constrains derived from the Saggitarius stream that favor $b/a \approx 0.97$ and $c/a \approx 0.44$.

Key words: galaxies: evolution — galaxies: formation — galaxies: haloes — dark matter

1 INTRODUCTION

The understanding of our Universe as a whole is greatly influenced by accurate observations and modeling of our Galaxy. Explaining the matter budget and kinematical state of the Milky Way (MW) is equivalent to figuring out its formation process in a cosmological context. As a first approximation, the MW morphology and separation into global kinematically coherent components, such as its disk and bulge, can be used to support the existence of a Dark Matter (DM) component to explain its dynamics around the solar neighborhood (Olling & Merrifield 2000a; Sofue et al. 2009; Catena & Ullio 2010; Bovy & Rix 2013; Iocco et al. 2015).

A more detailed description of the full three-dimensional MW gravitational potential is possible through the interpretation of fossil records of stellar streams. These remanents, resulting from infalling globular clusters or satellite galaxies that got tidaly disrutpted by the gravitational potential of the Milky Way, allow in principle tighter constrains on the shape of the dark matter halo in outter regions of our Galaxy (Johnston 1998; Helmi & White 1999; Tremaine 1999).

The observational constraints on the gravitational potential shape can then be confronted against the expectations from different galaxy formation models in an explicit cosmological context. For instance, in the current dominant paradigm of Cold Dark Matter (CDM) dominated Universe galaxies are expected to be hosted by triaxial DM halos. To what extent the CDM expectations are born out by observations in our Galaxy? Can the MW's DM halo shape be considered typical or atypical in a cosmological context?

These two questions have been difficult to address because for a long time it was difficult to produce realistic galactic disks within the CDM context. The success of such enterprise has been the result of high numerical resolution and the understanding that baryonic effects such as stellar feedback and black hole feedback play an important role in forming a galactic disk resembling the Milky Way.

Along the way numerical experiments show that the baryonic effects also impact the dark matter halo shape making the halo rounder than it otherwise be in a dark matter only simulation (Dubinski 1994; Debattista et al. 2008;

⋆ E-mail: jd.prada1760@uniandes.edu.co

Kazantzidis et al. 2010; Abadi et al. 2010; Bryan et al. 2013; Chua et al. 2019; Artale et al. 2019). High resolution simulations have also allowed detailed studies of the alignment between the stellar disk and the dark matter halo Bailin et al. (2005); DeBuhr et al. (2012); Debattista et al. (2013); Gómez et al. (2017).

Observational constraints of the dark matter halo have been in conflict during the last decade. Some studies prefer oblate configurations at small distances around $\leq$ 20 kpc (Law & Majewski 2010; Bovy et al. 2016; Loebman et al. 2012; Olling & Merrifield 2000b; Banerjee & Jog 2011) while others tend towards more triaxial and prolate configurations on the outter distances $\geq$ 20 kpc (Vera-Ciro & Helmi 2013; Law et al. 2009; Banerjee & Jog 2011; Deg & Widrow 2013). Some other studies are inclined towards prolate configurations even at the inner parts of the halo (Bowden et al. 2016), and although it previously seemed that a triaxial DM halo on the outskirts would be necessary to fully explain the characterization of the Sagittarius stream (Law et al. 2009), recent studies questioned this claim by reporting inconsistencies with narrow stellar streams Pearson et al. (2015) or finding that the relaxation of other constraints may make this claim unnecessary Ibata et al. (2013) axisymmetrical to ensure the stability of a hydrodynamical disk embeded in a static DM halo.

In this paper we address the question of measuring the shape of the DM halo in MW type galaxies from state-of-the-art simulations from the Auriga project. These simulations have large enough numerical resolution, and explicit cosmological context and an appropriate feedback physics to produce realistic MW disks. This paper is structured as follows. In Section 2 we present the most relevant details of the simulations, in Section 3 we present the method that we use to measure the DM halo shape. In Section 4 we present our results focusing on the radial shape trends at $z = 0$ and the alignments with the stellar disk. We discuss our results in Section 5 to place them into the context of other numerical work, explore correlations of the shape with baryonic properties in the disk and finally make a direct comparison against observational constraints for the MW's dark matter halo shape. We finalize with our conclusions in Section 6.

2 NUMERICAL SIMULATIONS

The Auriga project offers cosmological zoom in simulations of MW-sized dark matter halos in a ΛCDM cosmology. This simulations come in two versions: dark matter only (DMO) and baryonic physics including magetohydrodynamics (MHD). A detailed description of the simulations and their disk properties can be founc in (Grand et al. 2017), here we summarize its main features.

The objects in the simulations were selected from a set of 30 isolated halos in the Evolution and Assembly of GaLaxies and their Environments (EAGLE) project (Schaye et al. 2015). These halos were randomly selected from a sample of the most isolated halos at $z = 0$ whose virial mass M_{200} was between $10^{12} M_\odot$ and $2 \times 10^{12} M_\odot$. The cosmological parameters in these simulatins correspond to $\Omega_m = 0.307$, $\Omega_b = 0.048$, $\Omega_\Lambda = 0.693$ and a dimensionless Hubble parameter $h = 0.6777$ (Planck Collaboration et al. 2014)

The selected halos were re-simulated at higher resolution by applying a zoom-in technique with varying physical realism using the moving-mesh AREPO code that includes gravity, ideal magnetohydrodynamics, phenomenological descriptions for star formation, chemical enrichment from supernovae and its stellar feedback. The simulation also follows the formation and evolution of black holes together with the Active Galactic Nuclei feedback (Springel 2010; Pakmor & Springel 2013).

The 30 zoom-in halos have a dark matter particle mass of $\sim 3 \times 10^5\,\mathrm{Mpc}_\odot$ while the barynic mass resolution is $\sim 5 \times 10^4\,\mathrm{Mpc}_\odot$. The softening lenght for gravitational force computation for stellar particles and high-resolution dark matter particles is fixed to be 500 h^{-1} pc in comoving coordinates up to $z = 1$, and 396 pc in physical coordinates afterwards. The gravitational softening lenght for gas cells changes with the mean cell radius but is limited to be larger than the stellar softening lenght and 1850 pc physical. From now on we refer to the haloes simulated with baryonic physics as the MHD sample and to the haloes simulated with dark matter only as the DMO sample.

3 HALO SHAPE MEASUREMENT

The DM halo shape at a fixed radius is an estimate of either the isopotential or isodensity surfaces. Observational inference models usually estimate the isopotential contours which are probed by tracers (gas, stars), while simulations work with the isodensity contours which can be directly calculated from particle positions. Furthermore, the density contours in thin shells are very sensitive to the presence of small satelites. For this reason we measure the shape by taking volume-enclosed particles, rather than shell-enclosed. This method yields results in good agreement to the isodensity contours for radii $leq140$ kpc as explored by (Vera-Ciro et al. 2011).

In particular, we measure the shape using the reduced inertia tensor (**?**),

$$I_{ij} = \sum_k \frac{x_k^{(i)} x_k^{(j)}}{d_k^2}, \tag{1}$$

where the particle positions are measured from the minimum of the gravitational potential in each halo and each is weighted by the k-th particle distance $d_k^2 = x_k^2 + y_k^2 + z_k^2$.

The diagonalization of this tensor yields the eigenvectors and eigenvalues that represent an ellipsoidal dark matter halo. The axis lenghts of this ellipsoid $a \geq b \geq c$ are the square root of the $\mathbf{I}$ eigenvalues and the direction of the principal axis are the corresponding eigenvectors

We start the calculations taking into account particles within a sphere of radius R and then recharacterize the triaxial parameters by taking into account particles within an ellipsoid of semi-axes $r, r/q, r/s$ and re-scaled distance $d^2 = x^2 + (y/q)^2 + (z/s)^2$, where $q = b/a$ and $s = c/a$ are the previously calculated axial ratios. We repeat this process until the average deviation of semi-axes is less than 10^{-6}. After convergence we define a unique radius R as the geometrical mean of the axial lenghts $R = (abc)^{1/3}$. We use this radial coordinate R to parameterize the spatial changes in halo shape we report in the following sections.

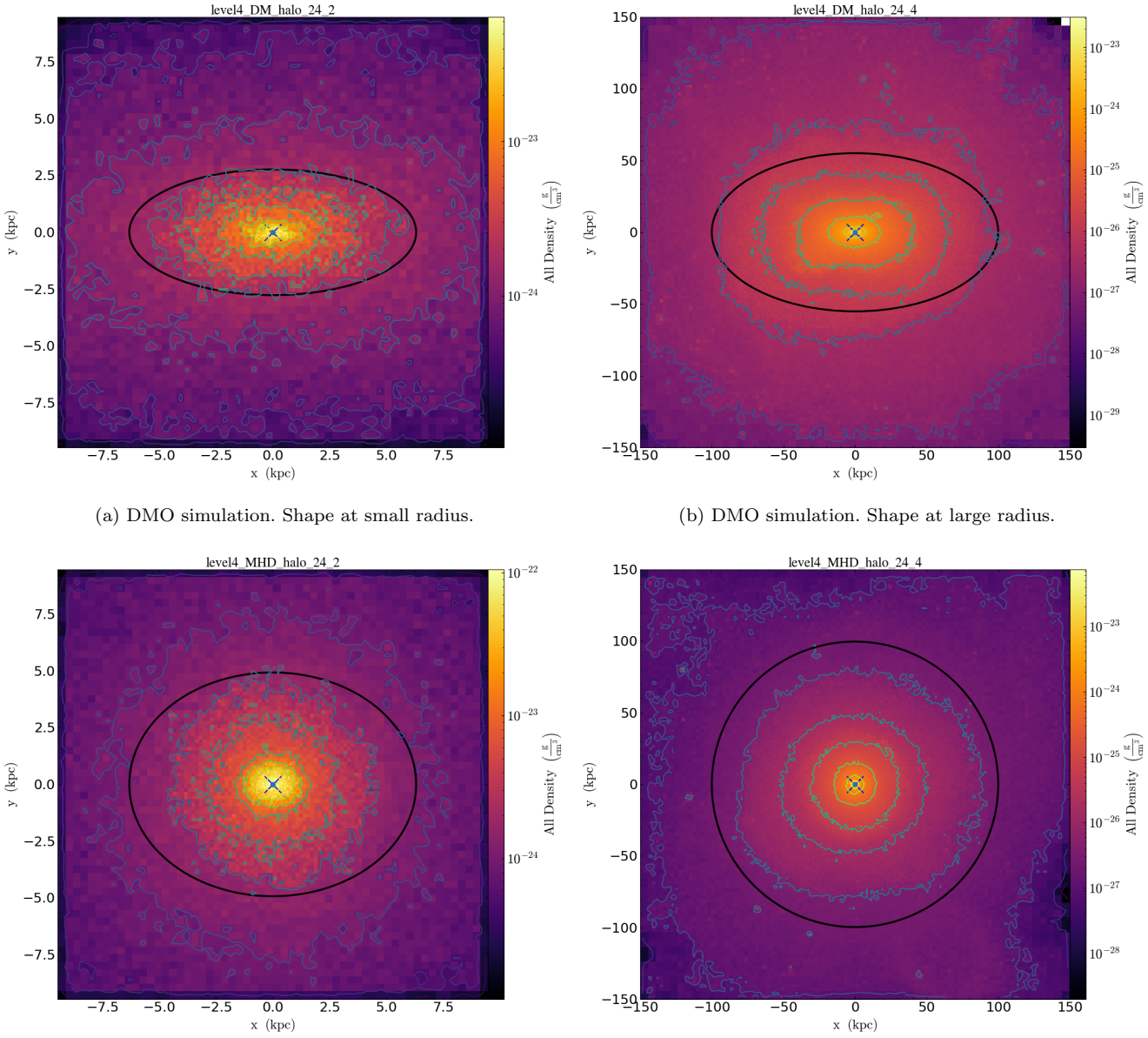

(a) DMO simulation. Shape at small radius.

(b) DMO simulation. Shape at large radius.

(c) MHD simulation. Shape at small radius.

(d) MHD simulation. Shape at large radius.

Figure 1. DM density in logarithmic scale within a slice of one tenth of the virial radius in width. The cut is perpendicular to the short axis of the inertia tensor ellipsoid. The black ellipses show the results of the fitting procedure. Upper panels correspond to DMO simulations, lower panels to MHD simulations. All cases correspond to `Level4` resolution. Left panels show data at small radii, while right panels at large radii. This halo showcases the most noticeable effect in all halos across the Auriga simulations: DM halos are rounder at all radii after baryonic physics is included.

This is the same method used to estimate the halo shape in the DM-only Aquarius simulations (Vera-Ciro et al. 2011).

Following the convergence criterion by **?** we restrict the sampling of the ellipsoidal parameters to radii between $\sim$ 2kpc and R_{200}, where R_{200} correspond to the radius enclosing a sphere with 200 times the critical density of the Universe. On average, over the 30 halos in the `Level4` sample $R_{200} = 230 \pm 15$kpc. For `Level3` halos we go down to distances of ~ 0.2 kpc.

4 RESULTS

4.1 Radial trends at $z = 0$

In the DMO sample we find that halos are rounder with increasing radius. The upper panels in Figure 1 illustrate this effect. The contours show a projected DM slice while the ellipsoid corresponds to the full 3D shape determination. There we see a highly ellipsoidal halo shape at radii $\sim$ 3kpc that becomes less triaxial at $\sim$ 50 kpc.

We summarize this trend in Figure 2 by plotting the results of all the 30 halos in the DMO sample. The left panel

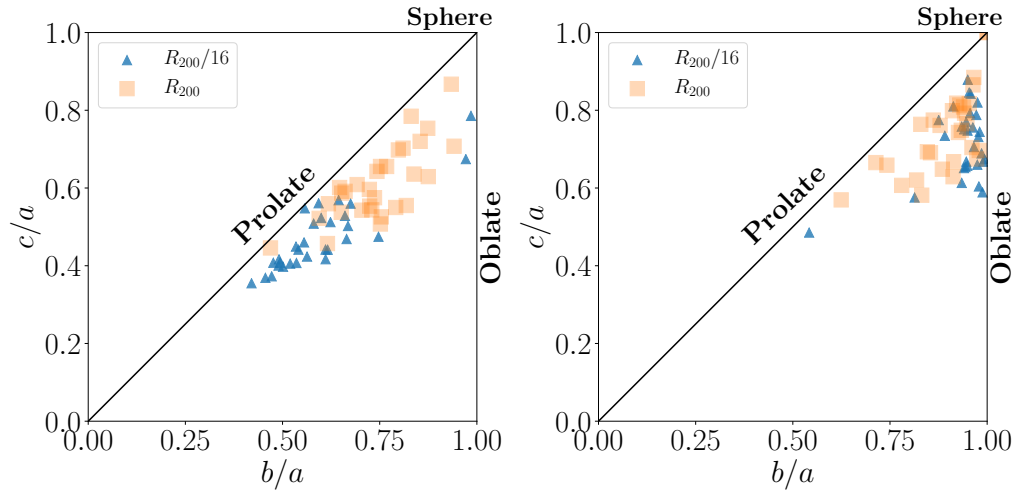

(a) DMO simulations. (b) MHD simulations.

Figure 2. Axial ratios for all halos in the simulation. Left/right panels correspond to DMO/MHD simulations, respectively. Triangles (squares) represent the measurements at $R_{200}/16$ (R_{200}) which correspond to physical distances of 14 ± 1 kpc (230 ± 15 kpc) respectively. Here we can visualize three main trends for the whole halo population. First, in DMO simulations halos are rounder in the outskirts than in the inner part. Second, halos in MHD are rounder than its DMO counterparts. Third, halos in MHD are less triaxial in the inner regions than in the outskirts.

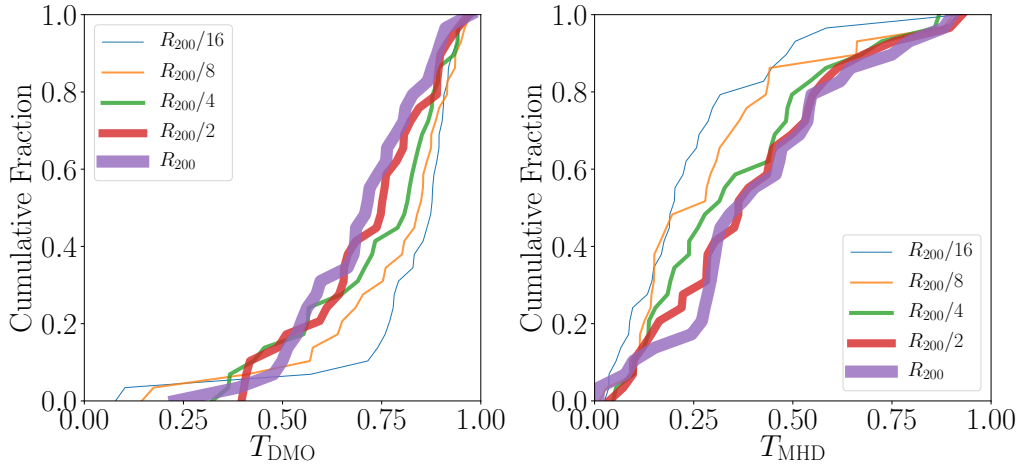

(a) DMO simulations. (b) MHD simulations.

Figure 3. Cumulative distribution for the triaxiality at five different radii. Right/left panel correspond to DMO/MHD simulations, respectively. In DMO simulations the median triaxiality at all radii is larger than 0.5; only for 20% the triaxility is smaller than 0.5. Furthermore, the triaxility increases as one moves towards the inner part of the halo. In MHD simulations the situation is reversed. The median triaxility at all radii is smaller than 0.5. Moving towards the stellar disk the triaxility decreases towards a median value of $T = 0.15$.

shows every halo in the c/a-b/a plane at two different radii $R_{200}/8(\sim 20\text{kpc})$ and R_{200}. The outer part of the halo is systematically rounder than its inner region. Nevertheless the halo shape can still be considerated to be prolate at all radii. These plots confirm the results already reported in the literature (Vera-Ciro et al. 2011).

A different picture presents itself in the MHD sample. There all halos become rounder at all radii than its DMO counterpart. The lower panel in Figure 1 can be directly compared to its MHD counterpart; there we observe how at large radii the halo becomes almost spherical. The right panel in Figure 2 shows the results for the 30 halos in the MHD sample. This time the bulk of the halos can be considered oblate and close to spherical.

In Figure 3 we summarize the results at different radii using the cumulative distributions for the triaxility parameter T defined as

$$T = \frac{a^2 - b^2}{a^2 - c^2}. \quad (2)$$

The left panel of this Figure shows that in the DMO sam-

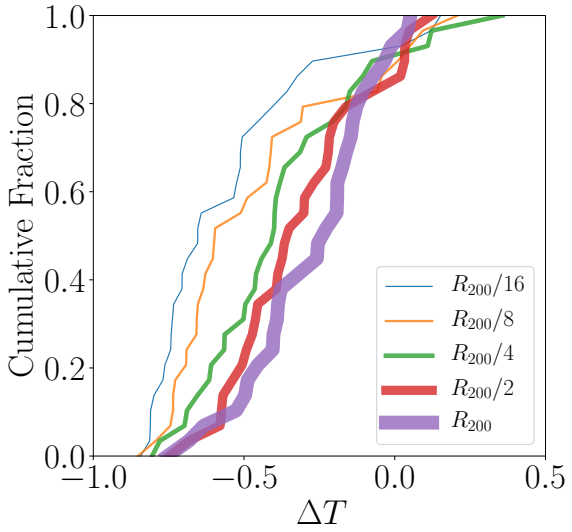

Figure 4. Cumulative distribution for the change in triaxility $\Delta T = T_{\rm MHD} - T_{\rm DMO}$ for the same radii used in Figure 3. At the virial radius all the halos become less triaxial in the MHD simulations. The change in triaxility becomes stronger in the inner regions of the dark matter halo.

ple the triaxility has a median larger than 0.5 at all radii, furthermore this median value increases as we move towards the inner part of the halo. The right panel shows the exact complementary picture in the MHD sampe. There the median triaxility is alwas smaller than 0.5 and this triaxility is smaller as we move closer to the galactic disk.

To quantify to what extend the global effect of decreasing triaxility in MHD simulations compared to the DMO sample holds for individual halos. We compute $\Delta T \equiv T_{\rm MHD} - T_{\rm DMO}$ the difference between the triaxility in the MHD and the DMO simulation for each individual halo. Figure shows the cumulative distribution at the same radii as in Figure .

4.2 Alignments with the stellar disk

A common assumption in observational models of the MW DM halo is that its minor axis is perfectly aligned with the stellar disk minor axis. Although it is a reasonable assumption to guarantee the stability of the galactic disk in simplified models of isolated galaxies, this might not hold in an explicit cosmological context. To examine the degree of validity of this assumption we study in this section the alignment between the eigenvectors of the inertia tensor of stellar particles within $0.1R_{200}$ ($\sim 23 \pm 2$ kpc) and the eigenvectors of the dark matter halo shape. All the measurements are done at $z = 0$.

In Figure 5 we summarize our main results regarding these alignments with the halo shape measured at five different radii. The upper row shows the alignment of the halos in the DMO simulations with the stellar disk in the MHD simulations. The main objective of this measurement is to calibrate the radial evolution of the DM halo shape. We find that the DM shape remains constant with radius.

The lower row in Figure 5 shows the alignments with the halo in the MHD simulations. This time the halo shape changes and twists at different radii. However around the radius of $0.25R_{200}$ there is an alignment almost perfect between the shapes of the stellar disk and the dark matter halo. Above and below this radius there are halos with a lower degree of alignment. Across the three different alignments we measure we verify that the strongest one is indeed the one between the two minor axis.

Statistically the strongest missalignment is found with the halo shape at a radius of $R_{200}/16 \sim (14 \pm 1)$ kpc. At this radius the mean angle and its standard deviation between the two minor axis is 18 ± 21 degrees, with one extreme case (`Au-4`) where the angle is close to 78 degrees. In contrast at $0.25R_{200}$ the angle between the two axis is 2 ± 3 degrees without any extreme outlier.

5 DISCUSSION

The first effect that we put in evidence in this paper is the effect of baryons in producing rounder DM halos.

The strength of the change depends on the numerical resolution, the method to resolve the hydrodynamics and the models describing star formation and stellar feedback (Debattista et al. 2008; Bryan et al. 2013; Butsky et al. 2016; Chua et al. 2019; Artale et al. 2019). The key concept unifying these results is that the baryon distribution influences and correlates with the dark matter halo shape. Here we find that the broad tendency is that massive stellar disks correlate with spherical dark matter distributions.

In order to explore this idea in the Auriga simulations we quantify the correlation between halo shape with baryonic disk properties. Looking into the measurements already reported by Grand et al. (2017) and Pakmor et al. (2017) we find three baryonic quantities that have the strongest correlation with DM halo triaxiality: the central gas density in a sphere of radius 1kpc, the disk to total mass ratio and the optical radius.

Figure 7 shows the correlations of these quantities with the triaxility at five diferent radii. We use the Spearmen's rank correlation coefficient to quantify the correlation strength. We find that the strongest correlations are found with the halo shape measured at radii smaller than $0.12R_{200} \sim 28$kpc, which is close to the upper limit of the disk optical radius among our simulation sample. The trend is such that halos with large triaxiality correlate with high gas density and stellar disks with low mass and small size. In turn, massive and large stellar disks within a low density gas environment correlate with low halo triaxiliaty.

Our second results deals with the disk-halo shape alignment as a function of radius. In concordance with previous results in DM only simulations we find that the shells of halo shape are well aligned at different radii. However, in the presences of baryons these shells twist as a function of radius. At a radius of $0.25R_{200} \approx 56$ kpc the alignment between the stellar disk and the dark matter halo is almost perfect and degrades at other radii. This twisting effect, the change of disk-halo alignment as a function of radius, is robust across our sample of 30 halos at all radii. However, its strenght is not the same for all galaxies and strongly correlates with halo triaxiality measured at $0.12R_{200}$.

Bailin et al. (2005) studied the disk halo alignmnent as a function of radius. Gómez et al. (2017) studied this in

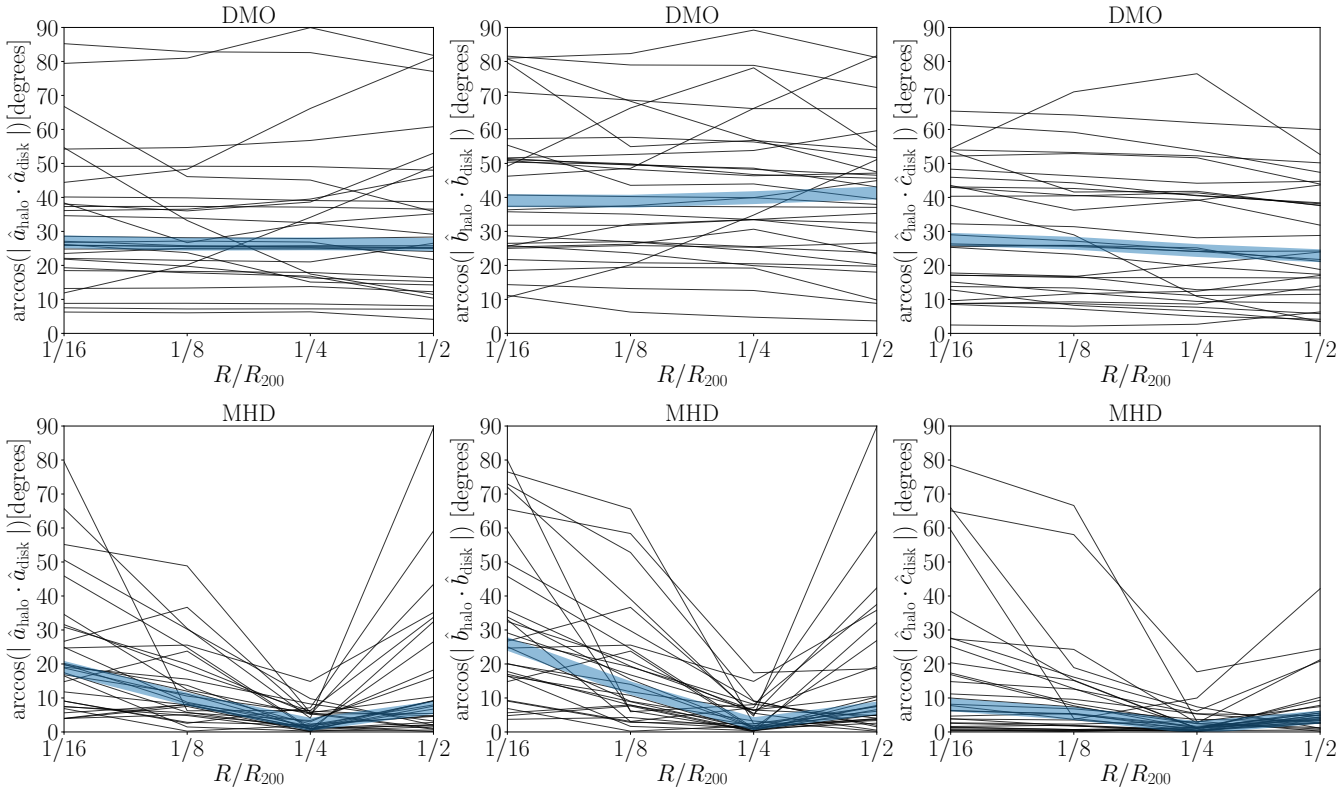

Figure 5. Angles between the principal axis of the halo shape and the principal axis of the stellar disk in the MHD simulations at four different radii $\leq 0.5R_{200}$. Thin lines correspond to each one of the thirty halos in our sample, while the thick line traces the median value. Each panel compares the alignment of the corresponding major/middle/minor axis both in the halo and the stellar disk. In the upper row the haloes come from the DMO simulation, showing that the ellipsoids describing the shape are constant as a function of radius for the most part of the sample. In the lower row the haloes come from the MHD simulation providing a self-consistent comparison with the stellar disks. In this case the dark matter shells twist in all the halos. The degree of this twisting is different in each halo. Interestingly, an almost perfect halo-disk alignment happens across the sample at an intermediate radius of $0.25R_{200}$ (56 ± 4kpc).

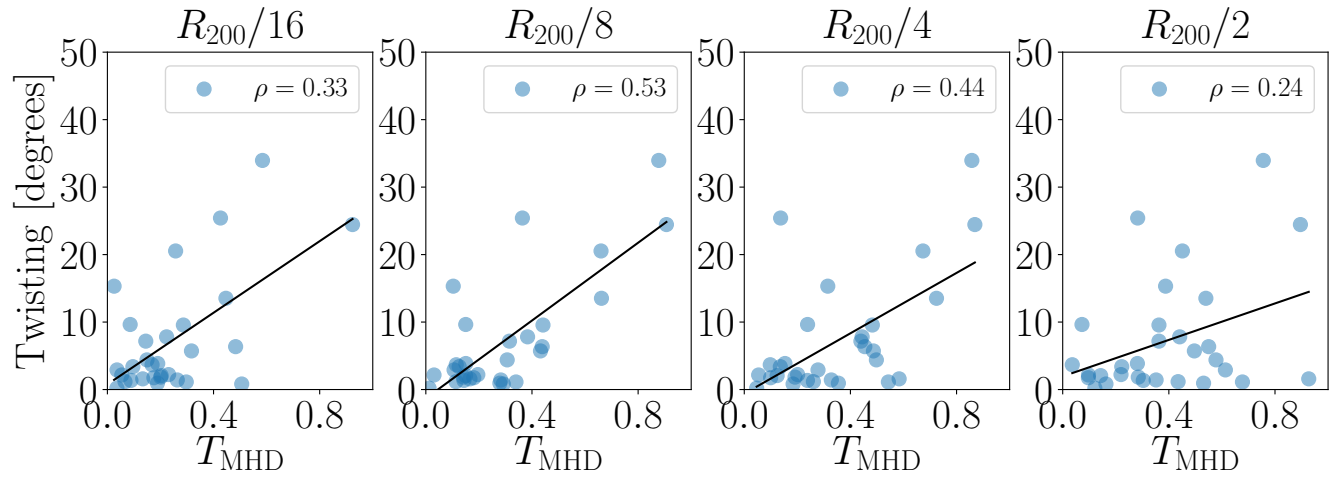

Figure 6. Changse of angle alignment of the dark matter halo and stellar disk at two different radii ($R_{200}/16$ and $0.25R_{200}$) as a function of the baryonic disk properties already explored in Figure 7. Figure 5 showed that maximum alignment occurs at $0.25R_{200}$ while in the inner regions ($R_{200}/16$) considerable missalignments occurr. at different radii and baryonic disk properties. The label with the ρ value corresponds to the SpearmanâĂŹs rank correlation coefficient.

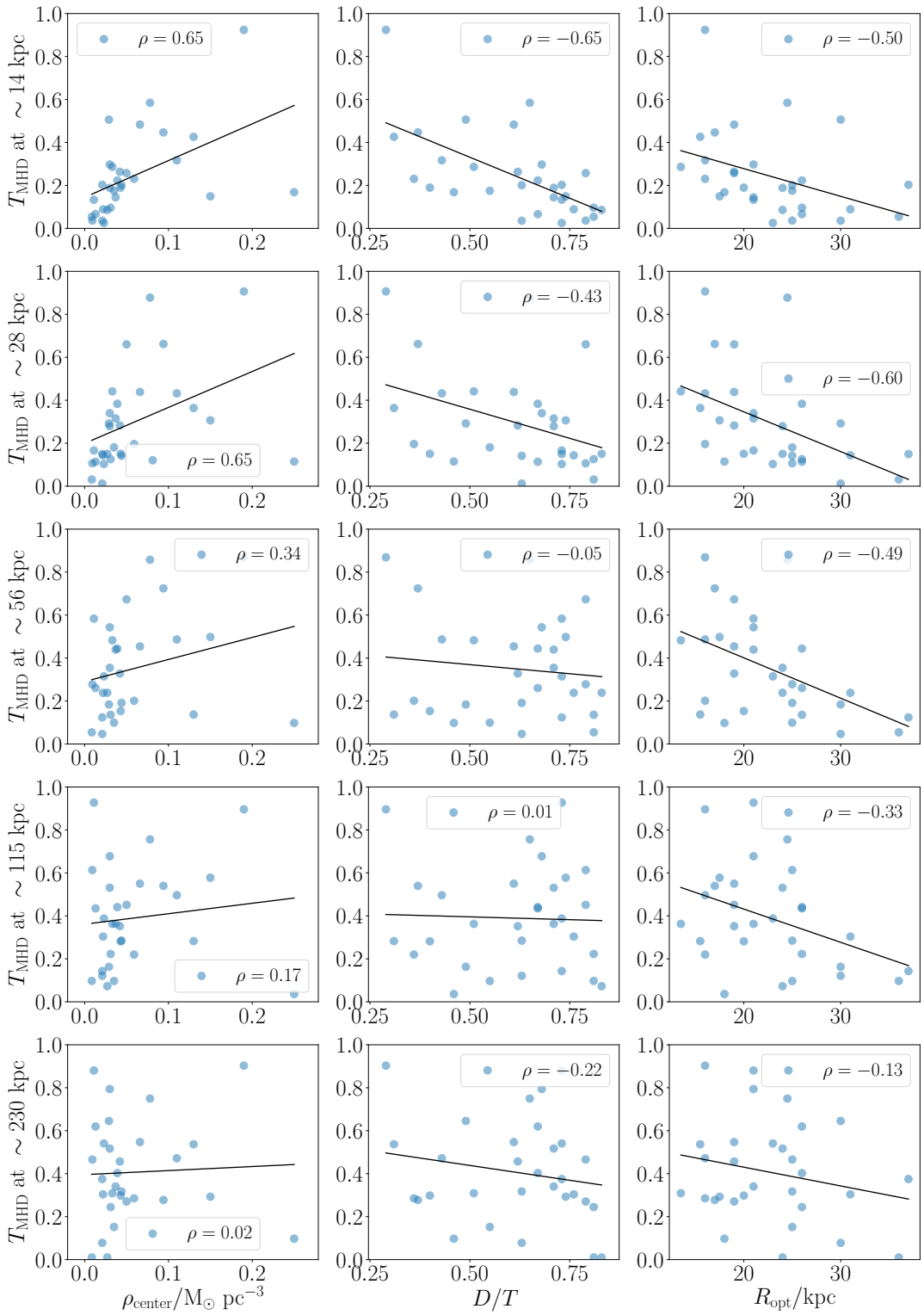

Figure 7. Correlations between the halo triaxility at different radii and baryonic disk properties. The label with the ρ value corresponds to the Spearman's rank correlation coefficient. The line is the best linear minimum squares fit. The x-axis in the first column is the gas density at the center of the galaxy with in a sphere of radius 1 kpc (Pakmor et al. 2017); the second column shows the disk to total mass ratio and the last column includes the disk optical radius defined to be the radius at which the B-band surface brightness drops below 25 mag arcsec^{-2} (Grand et al. 2017). The largest correlations are found for the two smaller radii and dilute as one approached R_{200}. Large and massive stellar disks with a low gas content are correlated with low dark matter triaxilities.

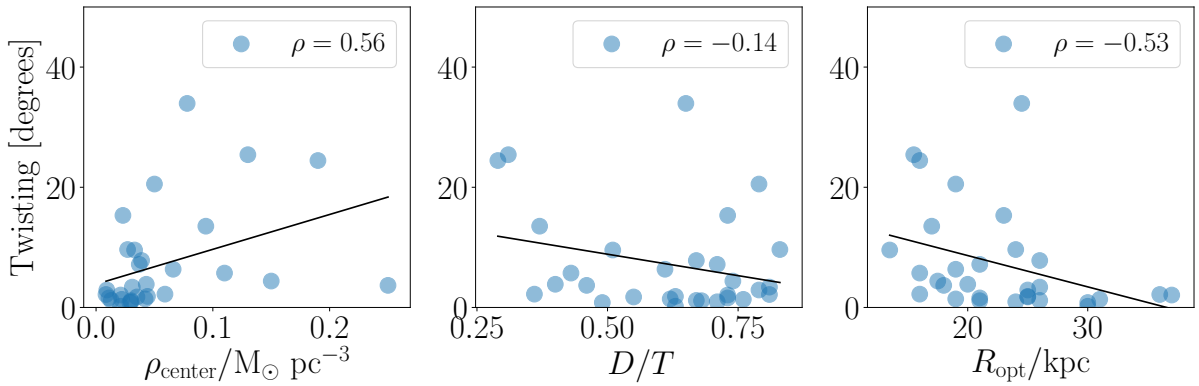

Figure 8. Changse of angle alignment of the dark matter halo and stellar disk at two different radii ($R_{200}/16$ and $0.25R_{200}$) as a function of the baryonic disk properties already explored in Figure 7. Figure 5 showed that maximum alignment occurs at $0.25R_{200}$ while in the inner regions ($R_{200}/16$) considerable missalignments occurr. at different radii and baryonic disk properties. The label with the ρ value corresponds to the SpearmanâĂŹs rank correlation coefficient.

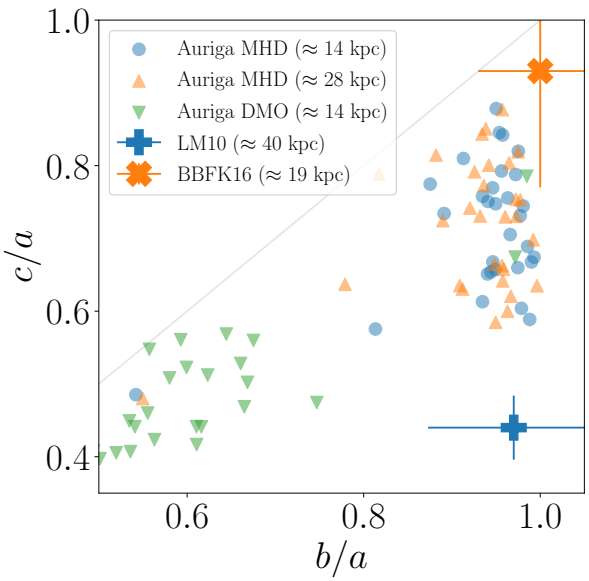

Figure 9. Comparison of our results against other simulations by Chua et al. (2019) (Illustris) and observational constraints for the dark matter halo shape in the Milky Way by Law & Majewski (2010) (LM10) and Bovy et al. (2016) (BBFK16). We report our results in the MHD simulations in such a way as to bracket the radii in the other estimates. We find that our results are broadly consistent with the Illustris simulations given the broad dispersion in both data sets. The consistency with the constraints by Bovy et al. (2016) is marginal, only 1/5 of the halos in our sample seem to be consistent within the observational reults. The result by Law & Majewski (2010) would place the Milky Way halo as an atypical object in the Λ CDM context.

Auriga. Debattista et al. (2013) reported a similar twisting effect, but only at radii smaller than the disk radius. At radii larger than the disk radius, they find, the dark matter shells stop twisting. Jing & Suto (2002) also reported shell alignment twisting in their dark matter only simulations as measured in the direction changes of large and medium shape axis. They only had three high resolution MW-like halos (with $\sim 10^6$ inside the virial radius) and could not make a statistical statement about the impact of this effect. However, they the twisting as an artifact resulting from high values of the c/b ratios that make the determination of the medium axis boisy. Could then high triaxility values explain the twisting as a result of erratic axis directions? If the triaxiality were the main culprit behind the twisting, the correlation between the two quantities should be constant at every radii. In Figure 8 we already showed that this correlation strongly depends on radius, we conclude that high triaxiality values cannot be the full explanation. Furthermore the twisting happens in such a way that it allows an almost perfect alignment between the stellar disk at 0.1R200 and the halo shape measured at $0.25R_{200}$

We now use the results reported by Law & Majewski (2010) and Bovy et al. (2016) to place our results in an observational context. Law & Majewski (2010) used observations of the Sagittarius tidal stream to constrain the shape of the gravitational potential. Their point of depart is that previous studies that assumed an axisymetric galactic potential were not able to fit all the available dynamic constraints for the Sagittarius stream, therefore making necessary the use of a rigid triaxial potential with coaxial potential ellipsoids for the dark matter component. Their results constrain the triaxility of this potential component. They also translate ther results into a triaxiality of the density contours (that could be compared against our results) to be $(c/a) = 0.44$ and $(b/a) = 0.97$ at a radius of $\sim$ 40kpc. They do not report any uncertainties for these two values. Looking at their plots for the quality of fit criterion as a function of dark halo axial scales (their Figure 5), we choose a conservative 10% relative uncertaintyy One surprising element in their results is that the major axis of the halo shape is perpendicular to the stellar disk plane.

The results by Bovy et al. (2016) have the same general approach but use instead the GD-1 (Grillmair & Dionatos 2006) and Pal 5 (Odenkirchen et al. 2009) streams to constraint the shape of the dark matter component of the galacic halo potential. They use general models with many degrees of freedom for the galactic potential in order to measure to what extent these two streams are sensitive to the

triaxiality of the dark matter halo component. The DM component is written directly as a triaxial density profile with coaxial ellipsoids and the corresponding potential is found by numerical integration. They find that the width of the Pal 5 stream constraints $b/a \approx 1$ and therefore fix it to be $b/a = 1$ exactly. Using that value they report their most stringent constrain of $c/a = 0.93 \pm 0.16$ at a radius of $\approx$ 19kpc from the galactic center.

Our Figure shows an explicit comparison in the c/a-b/a plane of our results in MHD simulations against the results by LM10 and BBFK16. We find six MHD halos with $b/a < 0.93$ and $c/a > 0.77$ that could be considered consistent with their shape constraints by BBFK16, while only one outlier DMO halo is consistent with those constraints. In contrast, none of the simulated halos (MHD nor DMO) is consistent with the LM10 results. The change of triaxility with radius in our simulations cannot account for these two extremely different shape constraints at different radii.

The results by LM10 could then place the dark matter halo of our Milky Way as an extreme outlier in the Λ CDM model. This extreme prolateness also correlates with the extreme triaxiality of the 11 classical satellites of the MW ($c/a \approx 0.2$, and $b/a \approx 0.9$) with an spatial distribution also oriented perpendicular to the MW plane, another highly unusual feature in the Λ CDM model (Forero-Romero & Arias 2018).

6 CONCLUSIONS

In this paper we measured the shape of thirty isolated Milky Way like dark matter haloes simulated in the Auriga project using the zoom-in technique. The Auriga project simulated these halos with two different setups: dark matter only (DMO) simulation and full magnetohydrodynamics (MHD) including star formation and feedback. We used the shape measurement algorithm by Allgood et al. (2006) on the dark matter halos of these two kinds of simulations to quantify the halo shape as a function of radius and the degree of aligment between the stellar disk and the halo.

We find that MHD halos are rounder than DMO halos every sampled radii. MHD halos tend towards more oblate shapes ($T < 1/3$) DMO halos tend towards more prolate shapes ($T > 2/3$). The rounding effect is more noticeable as one moves closer to galactic disk and strongly correlates with baryonic properties of the disk $\leq 0.10 R_{200} \approx$ 20kpc. More precisely, the triaxility is smaller for large and massive stellar disks with low gas densities in its core $\leq$ 1 kpc.

We also found that the alignment betwen the stellar disk and dark matter halo changes with the radius. At a radius of $0.25 R_{200}$ the alignment is almost perfect and degrades at smaller and larger distances. This alignment evolution implies a radial twisting between the ellipsoids describing the halo shape. We quantify this twist with the standard deviation of the angle between the two minor axis at radii below $\leq 0.5 R_{200}$ and find that it strongly correlates is with the disk size and the core gas mass density, there is only a weak correlation with the stellar mass in the disk.

We compared our results against two observational constraints for the dark matter halo shape of the Milky Way. The constraints are at two different radii and come from different observatinal tracers. We find that 20% halos in the MHD simulations are consistent with the constraints by Bovy et al. (2016) at $\approx$ 19kpc, while none of the halos, either in MHD or DMO, has some overlap with the shape constraints by Law & Majewski (2010) at $\approx$ 40kpc.

From the results presented in this work we advance the idea that the twisting shells in the density is a feature that deserves to be explored in the process of constraining shape parameters from tidal stream data. The inclusion of a parameterization describing this degree of twisting might relax the conflict between the observational constraints and the numerical results.

From the purely numerical point of view a better understading of the disk-halo alignment details will certainly require to study how the halo and the disk co-evolved as a function of time. Calibrating the effect of the cosmic web (both dark matter and gaseous) (Forero-Romero et al. 2014; Borzyszkowski et al. 2017; Ganeshaiah Veena et al. 2019) could also be required to gain a full picture of this behaviour.

ACKNOWLEDGEMENTS

This project has received funding from the European Union's Horizon 2020 Research and Innovation Programme under the Marie Skłodowska-Curie grant agreement No 734374.

REFERENCES

Abadi M. G., Navarro J. F., Fardal M., Babul A., Steinmetz M., 2010, MNRAS, 407, 435
Allgood B., Flores R. A., Primack J. R., Kravtsov A. V., Wechsler R. H., Faltenbacher A., Bullock J. S., 2006, MNRAS, 367, 1781
Artale M. C., Pedrosa S. E., Tissera P. B., Cataldi P., Di Cintio A., 2019, A&A, 622, A197
Bailin J., et al., 2005, ApJ, 627, L17
Banerjee A., Jog C. J., 2011, ApJ, 732, L8
Borzyszkowski M., Porciani C., Romano-Díaz E., Garaldi E., 2017, MNRAS, 469, 594
Bovy J., Rix H.-W., 2013, ApJ, 779, 115
Bovy J., Bahmanyar A., Fritz T. K., Kallivayalil N., 2016, ApJ, 833, 31
Bowden A., Evans N. W., Williams A. A., 2016, MNRAS, 460, 329
Bryan S. E., Kay S. T., Duffy A. R., Schaye J., Dalla Vecchia C., Booth C. M., 2013, MNRAS, 429, 3316
Butsky I., et al., 2016, MNRAS, 462, 663
Catena R., Ullio P., 2010, J. Cosmology Astropart. Phys., 8, 004
Chua K. T. E., Pillepich A., Vogelsberger M., Hernquist L., 2019, MNRAS, 484, 476
DeBuhr J., Ma C.-P., White S. D. M., 2012, MNRAS, 426, 983
Debattista V. P., Moore B., Quinn T., Kazantzidis S., Maas R., Mayer L., Read J., Stadel J., 2008, The Astrophysical Journal, 681, 1076
Debattista V. P., Roškar R., Valluri M., Quinn T., Moore B., Wadsley J., 2013, MNRAS, 434, 2971
Deg N., Widrow L., 2013, MNRAS, 428, 912
Dubinski J., 1994, ApJ, 431, 617
Forero-Romero J. E., Arias V., 2018, MNRAS, 478, 5533
Forero-Romero J. E., Contreras S., Padilla N., 2014, MNRAS, 443, 1090
Ganeshaiah Veena P., Cautun M., Tempel E., van de Weygaert R., Frenk C. S., 2019, MNRAS, 487, 1607

Gómez F. A., White S. D. M., Grand R. J. J., Marinacci F., Springel V., Pakmor R., 2017, MNRAS, 465, 3446
Grand R. J. J., et al., 2017, Monthly Notices of the Royal Astronomical Society, 467, 179
Grillmair C. J., Dionatos O., 2006, ApJ, 641, L37
Helmi A., White S. D. M., 1999, MNRAS, 307, 495
Ibata R., Lewis G. F., Martin N. F., Bellazzini M., Correnti M., 2013, ApJ, 765, L15
Iocco F., Pato M., Bertone G., 2015, Nature Physics, 11, 245
Jing Y. P., Suto Y., 2002, ApJ, 574, 538
Johnston K. V., 1998, ApJ, 495, 297
Kazantzidis S., Abadi M. G., Navarro J. F., 2010, ApJ, 720, L62
Law D. R., Majewski S. R., 2010, The Astrophysics Journal, 714, 229
Law D. R., Majewski S. R., Johnston K. V., 2009, The Astrophysical Journal Letters, 703, L67
Loebman S. R., Ivezić Ž., Quinn T. R., Governato F., Brooks A. M., Christensen C. R., Jurić M., 2012, ApJ, 758, L23
Odenkirchen M., Grebel E. K., Kayser A., Rix H.-W., Dehnen W., 2009, AJ, 137, 3378
Olling R. P., Merrifield M. R., 2000a, MNRAS, 311, 361
Olling R. P., Merrifield M. R., 2000b, MNRAS, 311, 361
Pakmor R., Springel V., 2013, MNRAS, 432, 176
Pakmor R., et al., 2017, MNRAS, 469, 3185
Pearson S., Küpper A. H. W., Johnston K. V., Price-Whelan A. M., 2015, ApJ, 799, 28
Planck Collaboration et al., 2014, A&A, 571, A16
Schaye J., et al., 2015, Monthly Notices of the Royal Astronomical Society, 446, 521
Sofue Y., Honma M., Omodaka T., 2009, PASJ, 61, 227
Springel V., 2010, Monthly Notices of the Royal Astronomical Society, 401, 791
Tremaine S., 1999, MNRAS, 307, 877
Vera-Ciro C., Helmi A., 2013, ApJ, 773, L4
Vera-Ciro C. A., Sales L. V., Helmi A., Frenk C. S., Navarro J. F., Springel V., Vogelsberger M., White S. D. M., 2011, MNRAS, 416, 1377